C. R. Physique 13 (2012) 889–898

Contents lists available at SciVerse ScienceDirect

Comptes Rendus Physique

www.sciencedirect.com

Structures and statistics of fluid turbulence / Structures et statistiques de la turbulence des fluides

Insight on turbulent flows from Lagrangian tetrads

Un éclairage sur les écoulements turbulents par l'étude de tétrades lagrangiennes

Alain Pumir [a,*], Aurore Naso [b]

[a] *Laboratoire de physique, Ecole normale supérieure de Lyon, CNRS and université de Lyon 1, 46, allée d'Italie, 69007 Lyon, France*
[b] *Laboratoire de mécanique des fluides et d'acoustique, Ecole centrale de Lyon, CNRS and université Lyon 1, 36, avenue Guy-de-Collongue, 69134 Ecully, France*

ARTICLE INFO

Article history:
Available online 6 November 2012

Keywords:
Turbulence
Flow structure
Scale dependence
Modeling

Mots-clés :
Turbulence
Structure de l'écoulement
Dépendance d'échelle
Modélisation

ABSTRACT

The insufficient understanding of the generation of small scales in turbulent flows results in serious impediment when trying to describe numerous physical problems, of natural or applied significance, and therefore, calls for new approaches. Here, we discuss the insight that can be gained by following the motion of a few points in a turbulent flow. This approach, which has shown its power in the context of the problem of dispersion of a passive scalar transported by turbulence, has led to new insight into some of the intriguing phenomena observed in turbulent flows, such as the alignment of vorticity with the eigenvectors of the rate of strain tensor. Recent work has focused on the motion of four points, forming initially a regular tetrad of size r_0. In particular, the modeling perspective inspired by the tetrad approach will be discussed here.

RÉSUMÉ

La connaissance trop partielle des mécanismes de génération des petites échelles dans les écoulements turbulents est une sérieuse entrave à la compréhension et à la prédiction quantitative de nombreux problèmes physiques, appliqués ou fondamentaux, et nécessite donc d'utiliser de nouvelles approches. Nous passons en revue les informations qui peuvent être obtenues en suivant le mouvement de quelques traceurs dans un écoulement turbulent. Cette approche, qui a montré son efficacité dans l'étude de la dispersion d'un scalaire passif transporté par la turbulence, a conduit à un éclairage nouveau sur quelques-uns des phénomènes surprenants observés dans des écoulements turbulents, tels que l'alignement de la vorticité avec les vecteurs propres du tenseur de taux de déformation. De récents travaux ont porté sur le mouvement de quatre particules formant initialement une tétrade régulière de taille r_0. Les perspectives de modélisation inspirées par cette approche sont présentées et discutées.

1. Introduction

Turbulent flows at high Reynolds numbers are characterized by the existence of a broad range of scales. In all applications and/or laboratory experiments, fluid is set into motion at large scales, through a variety of forcing mechanisms, and the

* Corresponding author.
E-mail addresses: alain.pumir@ens-lyon.fr (A. Pumir), aurore.naso@ec-lyon.fr (A. Naso).

1631-0705/$ – see front matter
http://dx.doi.org/10.1016/j.crhy.2012.09.001

energy injected in the flow is ultimately dissipated by viscosity at much smaller scales. The turbulent motion observed in the range of intermediate (inertial) scales merely transfers energy from large to small scales, and is therefore crucial to the understanding and modeling of the turbulence dynamics.

From a fundamental point of view, the observation of turbulent motion over a wide range of length scales suggests enticing scaling descriptions [1], which have been successful in many other scientific fields [2]. Early experimental work has rested on the measurement of (mostly) one velocity component of the velocity field in flows with a strong mean velocity [3], thus allowing to relate the time and space dependences of the velocity by the Taylor-frozen hypothesis approximation. Increasingly precise measurements of the scaling properties of the flow at very large Reynolds numbers have been obtained, and heuristic approximations have been proposed to describe the scaling exponents [4,5].

Beyond such a description in terms of scaling laws, much effort has been devoted to derive a proper theory directly from the equations describing the motion of the fluid, namely the Navier–Stokes equations:

$$\partial_t \mathbf{u} + (\mathbf{u}\cdot\nabla)\mathbf{u} = -\nabla p + \nu\nabla^2\mathbf{u} \tag{1}$$

$$\nabla\cdot\mathbf{u} = 0 \tag{2}$$

where ν is the viscosity, and p the pressure divided by the fluid density.

One of the cornerstones of turbulence theories has been provided by the (exact) relations, obtained directly from Eqs. (1), (2), which, under the mild assumption of local homogeneity and isotropy, relates the third moment of the component of the velocity difference along the x-axis, $\Delta u_x(r)$, to the distance r:

$$\left\langle \Delta u_x(r)^3 \right\rangle = -\frac{4}{5}\epsilon r + 6\nu\frac{\mathrm{d}}{\mathrm{d}x}\left\langle \Delta u_x(r)^2 \right\rangle \tag{3}$$

where ϵ is the dissipation of kinetic energy per unit mass of the fluid. Relatively few exact results have been obtained since Kolmogorov's seminal work (see, however, [6]).

The objective of deriving a consistent description of the statistical properties of the flow directly from the Navier–Stokes equations remains the objective of several approaches (including [7]).

The present work is aimed at describing several important properties of the velocity fluctuations. Our approach is arguably less ambitious, in the sense that it does not aim at obtaining a full theory, but mostly at expliciting some of the important properties of the flow. One of the important aspects of the so-called tetrad approach is that it is based on the simultaneous measurement of the position of several points in a turbulent flow, which is now feasible, thanks to the developments in Particle Tracking Velocimetry techniques.

In this short review, recent work, based on following the motion of several points in turbulent flows, will be reviewed, in particular concerning the modeling aspects.

2. The tetrad approach: motivations and elementary considerations

The approach discussed in this short review is based on the following remarks:

(i) In the Navier–Stokes equations, the velocity gradient tensor, $m_{ij} \equiv \partial_i u_j$, plays a crucial role. This remark is particularly important when trying to understand how small scales are generated via vortex stretching [8–10]. In the last decades, several models have been proposed to describe the Lagrangian dynamics of the **m** tensor [11–16].

(ii) Whereas a direct measurement of the velocity derivative in a turbulent flow remains, in view of the available experimental techniques, very difficult to carry out [17,18], recent progress in Particle Tracking Velocimetry allow us to investigate the motion of several particles in a turbulent flow, thus enabling a determination of the "perceived velocity gradient tensor", determined from a fluid tracer particle with respect to neighbor particles. Elementary geometric considerations, to be detailed below, show that the knowledge of the positions and velocities at $n \geqslant 4$ points are sufficient to determine the "perceived velocity gradient tensor", denoted **M** in the following. We will restrict ourselves here to the case of tetrads, i.e., $n = 4$ points.

Another motivation to follow more than one point in a turbulent flow comes from the remark that in general, multi-point correlation functions are a priori sensitive to possible structures in the flow. The work on the dynamics of a passive scalar in the presence of a mean gradient [19] has demonstrated that the three-point correlation function is indeed sensitive to the observed structures of the passive scalar field, namely the sharp jumps ("cliffs") seen both in experiments and in numerical simulations [20,21].

From a theoretical point of view, the statistical description of the velocity field of a turbulent flow is given by all the moments

$$\mathcal{M}_{i_1,i_2,\ldots,i_n}(\mathbf{x}_1,\mathbf{x}_2,\ldots,\mathbf{x}_n) \equiv \left\langle u_{i_1}(\mathbf{x}_1)u_{i_2}(\mathbf{x}_2)\cdots u_{i_n}(\mathbf{x}_n)\right\rangle \tag{4}$$

Attempts to obtain the moments $\mathcal{M}$ directly from the Navier–Stokes equations lead to the closure problem: moments of order n cannot be determined without previous knowledge of the $(n+1)$th moment. In this context, the study of the velocity

simultaneously measured at four points is merely a way to obtain directly information on the four point correlation function of the velocity field $\mathbf{u}$. In fact, the assumptions made while proposing a modeling approach are effectively equivalent to a closure of the moment hierarchy. The work described here however is based on a number of physical approximations, which can be justified, based on previous empirical knowledge [22], or confronted directly with direct numerical simulations (DNS) or experimental results.

One of the lessons learned while investigating the correlation functions for a passive scalar, in particular in the simplified case of the Kraichnan model [23–25] is that the Lagrangian point of view provides a very useful way to think about the correlation functions. In the case of a passive scalar, the scalar field is conserved along Lagrangian trajectories (up to the effect of the large scale forcing), which reduces the study of the correlation functions to the properties of the trajectories. Generalizing these ideas to the velocity field is one of the motivations, and challenges, of the approach reviewed here.

3. Tetrads and the perceived velocity gradient tensor: definitions and notation

3.1. Construction of the perceived velocity gradient tensor

The construction of the perceived velocity gradient tensor is based on the knowledge of the position, $\mathbf{x}_i$, as well of the velocity $\mathbf{u}_i$ of four tracer particles, simply moving with the flow velocity, $\mathbf{u}$:

$$\frac{\mathrm{d}}{\mathrm{d}t}\mathbf{x}_i(t) = \mathbf{u}\big(\mathbf{x}_i(t), t\big) = \mathbf{u}_i(t) \tag{5}$$

As we are considering a statistically homogeneous flow, the motion of the center of mass is immaterial; we therefore focus here to the motion of the four points with respect to the center of mass, or equivalently, to the relative motion between two vertices of the tetrad, $\mathbf{x}_i - \mathbf{x}_j$. More specifically, we introduce the reduced set of three vectors:

$$\begin{aligned}
\boldsymbol{\rho}_1 &= (\mathbf{x}_2 - \mathbf{x}_1)/\sqrt{2} \\
\boldsymbol{\rho}_2 &= (2\mathbf{x}_3 - \mathbf{x}_1 - \mathbf{x}_2)/\sqrt{6} \\
\boldsymbol{\rho}_3 &= (3\mathbf{x}_3 - \mathbf{x}_1 - \mathbf{x}_2 - \mathbf{x}_3)/\sqrt{12}
\end{aligned} \tag{6}$$

In the following, we denote the ath component of the vector $\boldsymbol{\rho}_i$ by $\rho_{i,a}$. The vectors $\boldsymbol{\rho}_i$ allow us to investigate the shape of the tetrads. Indeed, the geometry of the set of points can be conveniently parametrized by introducing the tensor $\mathbf{g}$, defined by its coordinates:

$$g_{ab} = \sum_{i=1}^{3} \rho_{i,a}\rho_{i,b} \tag{7}$$

The tensor $\mathbf{g}$ is symmetric, and as such, can be diagonalized in an orthonormal basis. Clearly, the three eigenvalues of $\mathbf{g}$, denoted g_i, are all positive; without loss of generality, we rank them in decreasing order: $g_1 \geqslant g_2 \geqslant g_3 \geqslant 0$. The trace of $\mathbf{g}$ is essentially equal to the square of the radius of gyration of the set of points.

The shape of the tetrads can be characterized by the ratios between the eigenvalues g_i. A very elongated, "needle-like" object, has an eigenvalue g_1 much larger than the two other eigenvalues. A flat, "pancake" like object, is characterized by a third eigenvalue, g_3 much smaller than the two larger values g_1 and g_2. We note in this respect that when the eigenvalue g_3 is very small, then, the four points defining the tetrad are nearly co-planar. In this case, not much information can be obtained concerning the velocity gradient in the direction perpendicular to the plane of the tetrad.

To define the perceived velocity gradient tensor, $\mathbf{M}$, we define, by analogy to $\boldsymbol{\rho}$, the velocities:

$$\begin{aligned}
\mathbf{v}_1 &= (\mathbf{u}_2 - \mathbf{u}_1)/\sqrt{2} \\
\mathbf{v}_2 &= (2\mathbf{u}_3 - \mathbf{u}_1 - \mathbf{u}_2)/\sqrt{6} \\
\mathbf{v}_3 &= (3\mathbf{u}_3 - \mathbf{u}_1 - \mathbf{u}_2 - \mathbf{u}_3)/\sqrt{12}
\end{aligned} \tag{8}$$

(we also denote the ath component of the vector $\mathbf{v}_i$ by $v_{i,a}$). With these variables, $\mathbf{M}$ is defined by minimizing the quantity:

$$Q = \sum_{i=1}^{3}\sum_{a=1}^{3}(v_{i,a} - \rho_{i,b}M_{b,a})^2 \tag{9}$$

with the constraint that $\mathrm{tr}(\mathbf{M}) = 0$. This leads immediately to a simple prescription for the determination of $\mathbf{M}$. Without the constraint of incompressibility, the solution of the minimization problem can be readily obtained:

$$\mathbf{M} = \boldsymbol{\rho}^{-1} \cdot \mathbf{v} \tag{10}$$

provided the matrix $\boldsymbol{\rho}$ is invertible. Special care has to be taken when the tensor $\mathbf{g}$ becomes singular, which happens when the four points of the tetrads are co-planar, and when the information obtained from the four points of the tetrads is not

sufficient to determine the velocity derivative in the direction perpendicular to the plane containing the points of the tetrad. In such a case, standard Single Value Decomposition methods can be readily used [26].

We are interested here in the evolution of tetrads initially regular, with equal distance between two vertices ($|\mathbf{r}_i - \mathbf{r}_j| = r_0$). Such configurations are characterized by one length scale only, which can be varied, thus allowing to characterize the properties of the velocity field as a function of scale. This provides insight on the properties of the flow, when studied at a given scale r_0. In particular, we expect that when r_0 is very small, of the order of (or smaller than) the Kolmogorov scale of the flow, $\eta \equiv (\nu^3/\epsilon)^{1/4}$, the properties of $\mathbf{M}$ will reduce to those of the velocity gradient tensor, $\mathbf{m}$. At very large scales, when r_0 is comparable, or larger than the integral length scale of turbulence, the matrix $\mathbf{M}$ is not expected to have any special property. Significant variations of the properties of $\mathbf{M}$ are therefore expected when the scale r_0 varies from dissipative to integral scales.

These changes are expected to have a significant impact both on the structure of $\mathbf{M}$, and on the evolution of the geometry of the tetrad. We consider these two aspects in the two following sections.

3.2. Characterization of the flow in terms of the perceived velocity gradient tensor

The construction of the perceived velocity gradient tensor allows us to obtain insight on the flow structure.

The matrix $\mathbf{M}$ is characterized by the two invariants R and Q, defined as $Q = -\frac{1}{2}\,\mathrm{tr}(\mathbf{M}^2)$ and $R = -\frac{1}{3}\,\mathrm{tr}(\mathbf{M}^3)$. In fact, the values of R and Q entirely determine the eigenvalues of $\mathbf{M}$. This is a consequence of the fact that the three eigenvalues of $\mathbf{M}$ are the three roots of the characteristic polynomial:

$$\lambda^3 + Q\,\lambda + R = 0 \tag{11}$$

Elementary considerations show that these roots can be either all real, or that one of them only can be real and the two other ones complex conjugate. Incompressibility imposes that the sum of these roots is equal to zero, but two cases can be distinguished: two roots (or their real part) can be positive and the third one negative, or two roots (or their real part) can be negative and the third one positive. Which configuration is seen depends on the sign of R, and of $\Delta = 4Q^3 + 27R^2$. Thus, it has been found interesting to investigate the probability distribution function (PDF) of R and Q. Previous studies, starting with [27], have shown that the PDF in the (R, Q) plane, constructed with the velocity gradient tensor, is strongly skewed, with a characteristic "tear-drop" shape.

It is also interesting to decompose $\mathbf{M}$ into its symmetric, $\mathbf{S} \equiv \frac{1}{2}(\mathbf{M} + \mathbf{M}^T)$, and its anti-symmetric components, $\frac{1}{2}(\mathbf{M} - \mathbf{M}^T)$, whose three non-zero components can be conveniently parametrized in terms of the vorticity $\mathbf{\Omega}$, defined such as $\Omega_a = \epsilon_{abc} M_{bc}$. The alignment of the vorticity with respect to the three eigenvectors of the strain, $\mathbf{S}$, associated with the three real eigenvalues λ_i sorted in decreasing order: $\lambda_1 \geqslant \lambda_2 \geqslant \lambda_3$, is also instructive about the structure of the turbulent flow.

4. Numerical and experimental results on tetrad dynamics

4.1. Tetrad geometry

To characterize the evolution of the tetrad geometry, we focus on the eigenvalues g_i of the tensor $\mathbf{g}$. By considering initially regular tetrads, the eigenvalues of $\mathbf{g}$ at time $t = 0$ are equal to each other, and $g_1 = g_2 = g_3 = r_0^2/3$ (with our conventions, see Eqs. (6), (7)). The problem of the geometry of tetrads can be viewed as a natural extension of the problem of Richardson dispersion. Indeed, turbulent motion not only leads to a separation of two neighbor particles, but also to a deformation of a set (cloud) of particles, which reflects the structure of the flow.

The deformation of the tetrads can be conveniently monitored by measuring the (dimensionless) ratio between eigenvalues. More specifically, the ratios

$$\hat{I}_1 = \frac{g_1}{g_1 + g_2 + g_3} \tag{12}$$

$$\hat{I}_2 = \frac{g_2}{g_1 + g_2 + g_3} \tag{13}$$

$$\hat{I}_3 = \frac{g_3}{g_1 + g_2 + g_3} \tag{14}$$

have been recently investigated, both in DNS [28,29,31] and in experiments [30], at Reynolds numbers up to $R_\lambda \approx 1000$ [31] (note that the sum $\hat{I}_1 + \hat{I}_2 + \hat{I}_3 = 1$).

At moderate Reynolds numbers, the early observations [28] have shown a strong flattening of the tetrads, in such a way that $\hat{I}_2$ decreases very fast, and tends to reach an asymptotic value at large times, when the size of the tetrad becomes larger than the integral size. One important remark is that the evolution of the deformation of the tetrad scales with the time $t_0 = (r_0^2/\epsilon)^{1/3}$, which is the characteristic time at scale r_0 in the Kolmogorov theory [30].

One of the questions one may ask in this respect is whether the deformation becomes statistically independent of r_0 when the range of scales becomes very large, or equivalently, when the Reynolds number $R_\lambda \to \infty$. Theoretical arguments supporting this possibility were presented in [28]. Suggestive evidence was provided by the numerical work at

$R_\lambda \lesssim 300$ [29]. The most recent simulation at $R_\lambda \approx 1000$ brings very strong evidence that at very high Reynolds number, the deformation of the tetrads becomes independent of time and scale provided that the separations between the vertices of the tetrads are all in the inertial range [31].

A very strong reduction of the third eigenvalue of $\mathbf{g}$, as measured by $\hat{I}_3$, Eq. (14), has also been observed in [29,31,30].

One of the most significant lessons of these studies is that strong deformation is occurring over a fraction of the Kolmogorov time scale in the problem, namely t_0. It is remarkable that the evolution seems to be to a large extend self-similar, in the sense that the various moments investigated so far seem to be functions of the ratio t/t_0. In the inertial range, at very large Reynolds numbers, the average of the ratio $\langle g_2/\operatorname{tr}(\mathbf{g})\rangle$ reaches a steady state, which suggests that the shape distribution reaches a steady state, reflecting the local structure of the turbulent flow. Last, it has been observed that tetrads tend to become strongly flattened with a significant probability, suggesting that the matrix $\mathbf{g}$ is in fact quite likely to be singular.

4.2. Evolution of $\mathbf{M}$: alignment of the vorticity and strain

One of the very puzzling observations concerning the small scale properties of turbulent flows concerns the alignment between vorticity, $\boldsymbol{\omega} \equiv \nabla \times \mathbf{u}$ and the rate of strain, $\mathbf{s}$, defined by $s_{ij} = 1/2(\partial_i u_j + \partial_j u_i)$ [32,35]. In fact, vorticity is known to grow due to vortex stretching, according to:

$$\frac{\mathrm{d}}{\mathrm{d}t}\boldsymbol{\omega} = \mathbf{s}\cdot\boldsymbol{\omega} + \nu\nabla^2\boldsymbol{\omega} \tag{15}$$

The growth of vorticity is due to the term $\mathbf{s}\cdot\boldsymbol{\omega}$ in Eq. (15). This term can be simply expressed in the basis of the three orthogonal vectors $\mathbf{e}_i$, $i = 1$, 2 and 3 that diagonalizes $\mathbf{s}$ (we assume that the eigenvalues of $\mathbf{s}$, λ_i, are sorted in descending order $\lambda_1 \geqslant \lambda_2 \geqslant \lambda_3$). A natural expectation would be that $\boldsymbol{\omega}$ grows mostly in the direction of $\mathbf{e}_1$, corresponding to the largest eigenvalue of $\mathbf{s}$. However, vorticity also induces a rotation of the eigenframe of $\mathbf{s}$ that counteracts its growth in the $\mathbf{e}_1$ direction [33,34]. This could explain the numerical results of [35–37], that show that vorticity preferentially aligns with $\mathbf{e}_2$ (which corresponds also predominantly to a positive value of λ_2). These properties concern the velocity *derivative* tensor, and have been confirmed many times numerically. Although accurate measurements of the velocity derivatives are very demanding in terms of spatial resolutions, experiments using multi-wire probes have confirmed the numerical observations.

The tetrad approach allows us to study the problem from another point of view. Namely, once the tetrad based matrix $\mathbf{M}$ has been determined, one can also study the vorticity $\boldsymbol{\Omega}$, associated with the anti-symmetric component of $\mathbf{M}$, and the rate of strain $\mathbf{S} = \frac{1}{2}(\mathbf{M} + \mathbf{M}^T)$.

As it was the case with the velocity derivatives, it has been found that the vector $\boldsymbol{\Omega}$ does not show any particular alignment with the eigenvector $\mathbf{e}_1$ of $\mathbf{S}$ corresponding to the largest eigenvalue. However, the dynamics of $\mathbf{M}$ obtained experimentally and numerically [38], shows that vorticity does tend to align with $\mathbf{e}_1$, although with a delay. To quantify this effect, the correlation function:

$$C_i(t) = \left\langle \left(\mathbf{e}_i(0)\mathbf{e}_{\Omega}(t)\right)^2 \right\rangle \tag{16}$$

was introduced, where $i = 1$, 2 or 3 refers to the eigenvalues of strain in decreasing order. In particular, the function $C_1(t)$ measures the alignment between $\mathbf{e}_1$ and $\boldsymbol{\Omega}$ at some later time. Direct numerical simulations, as well as results from laboratory experiments [38–40] do show a significant increase from $C_1 \approx 1/3$ at $t = 0$, up to a maximum of $C_1 \approx 0.43$ at $t \approx 0.25 \times t_0$. Remarkably, the curves representing the evolution of $C_1(t)$ superpose very well, once time has been expressed in units of t/t_0 [38]. Furthermore, the data show an almost perfect superposition of the probability distribution functions (PDF) of the cosine $(\mathbf{e}_1(0)\mathbf{e}_{\Omega}(t))$, at similar values of t/t_0, both at different values of r_0 at a fixed Reynolds number, and also at different Reynolds numbers [38,40]. As it was the case in the study of the deformation of tetrads, the quantities characterizing the alignment of vorticity with the eigenvector associated with the largest eigenvalue of strain thus all seem to evolve in a self-similar way as a function of t/t_0.

An appealing interpretation of these results, based on the notion of conservation of angular momentum, has been proposed to explain the observed alignment between $\mathbf{e}_{\Omega}(t)$ and $\mathbf{e}_1(0)$. The size of the tetrad increases most in the direction parallel to the largest eigenvector of the rate of strain tensor, $\mathbf{e}_1$, and much less in the two other perpendicular directions. Thus, the components of the tensor $\mathbf{g}$ in the directions parallel to the eigenvalue $\mathbf{e}_1$ of the rate of strain is much larger than the components parallel to $\mathbf{e}_{2,3}$. This implies that the projection of the moment of inertia tensor, familiar in the context of solid mechanics, and defined as:

$$\mathbf{I} = \operatorname{tr}(\mathbf{g})Id - \mathbf{g} \tag{17}$$

diminishes in the direction parallel to $\mathbf{e}_1$.

We notice that the angular momentum of small fluid volume contained in an individual tetrad is the product of the moment of inertia tensor $\mathbf{I}$ times the vorticity vector [38]. In the directions where the component of $\mathbf{I}$ diminishes, the component of vorticity has to increase in order to conserve angular momentum. Therefore, in the direction parallel to $\mathbf{e}_1$, where the eigenvalue of the tensor $\mathbf{I}$ decreases most, the component of vorticity is most amplified. Thus, conservation of angular momentum, together with the fact that the tetrad grows most in the direction of the eigenvector corresponding to

the largest eigenvalue of the rate of strain, leads to the alignment of vorticity with $\mathbf{e}_1$. It was indeed found that angular momentum conservation is indeed a good approximation for the evolution of tetrads in a turbulent flow [38].

Similar arguments for the amplification of vorticity had been suggested in the classical textbook [41]. In the case of *finite* tetrads studied here, however, the equations describing the evolution of the system are not known, preventing the casual use of simple models.

Further results concerning the alignment between vorticity and strain are discussed in [40], and suggest the interesting possibility that the dynamics of alignment of vorticity with the eigenvectors of strain could be essentially self-similar in the inertial range, at least at high enough Reynolds numbers.

5. Modeling issues

A model for the Lagrangian dynamics of $\mathbf{M}$ has been proposed by Chertkov, Pumir and Shraiman [22]. The so-called "tetrad model" is based on a particle representation of the velocity of four fluid particles. The model is formulated in terms of two coupled stochastic differential equations, modeling the evolution of $\mathbf{M}$, the coarse-grained velocity gradient tensor, along with the three vectors $\boldsymbol{\rho}_i$ $(i = 1, 2, 3)$, which describe the shape of the tetrad with respect to its center of mass,

$$\frac{\mathrm{d}M_{ab}}{\mathrm{d}t} + (1-\alpha)\big(M_{ab}^2 - \Pi_{ab}\,\mathrm{Tr}\big(\mathbf{M}^2\big)\big) = \eta_{ab} \tag{18}$$

$$\frac{\mathrm{d}\rho_{i,a}}{\mathrm{d}t} + \rho_{i,b}M_{ba} = \xi_{i,a} \tag{19}$$

$$\Pi_{ab} = \frac{k_{i,a}k_{i,b}}{\mathrm{Tr}(\mathbf{k}\mathbf{k}^{\mathbf{T}})} \tag{20}$$

where the matrix $\mathbf{k}$ is the inverse of $\boldsymbol{\rho}$. With the notation used here, the indices a, b, … refer to the spatial coordinates, whereas the indices i, j, … refer to the index of the vectors ("isospin"), as defined in Eq. (6). The deterministic parts of equations (18), (19) (left-hand side of the equations) represent the effects of the dynamics induced by scales of order $|\rho|$. The matrix $\boldsymbol{\Pi}$, defined by Eq. (20), is symmetric with a trace equal to 1; it provides a coupling of the geometry with the dynamics of $\mathbf{M}$. Lastly, the stochastic terms $\boldsymbol{\eta}$ and $\boldsymbol{\xi}$ in Eqs. (18), (19) represent the random effect of the small scales of motion. They are represented by Gaussian, white-in-time noise terms, with a scale dependence prescribed by dimensional considerations, consistent with Kolmogorov scaling,

$$\big\langle \eta_{ab}(0)\eta_{cd}(t)\big\rangle = C_\eta \delta(t)\frac{\epsilon}{\rho^2}\left(\delta_{ac}\delta_{bd} - \frac{1}{3}\delta_{ab}\delta_{cd}\right) \tag{21}$$

$$\big\langle \xi_{i,a}(0)\xi_{jb}(t)\big\rangle = C_\xi \delta(t)\sqrt{\mathrm{Tr}\big(\mathbf{M}\mathbf{M}^T\big)}\big(\delta_{ab}\rho^2\delta_{ij} - \rho_{i,a}\rho_{j,b}\big) \tag{22}$$

where $\rho^2 = \mathrm{Tr}(\boldsymbol{\rho}\boldsymbol{\rho}^T)$. The noise term acting on $\boldsymbol{\rho}$, $\boldsymbol{\xi}$, is assumed here to act only in the direction transverse to the nine-dimensional vector $\boldsymbol{\rho}$ which is not expected to be a significant restriction. The parameter α represents the effective reduction of the nonlinearity, already identified many times in simulations of the Navier–Stokes equations. It is represented here by a dimensionless parameter, satisfying $0 \leqslant \alpha \leqslant 1$. The two other parameters in the problem are the amplitudes of the noise terms: C_η and C_ξ.

The solution of this stochastic model, written as a set of 14 coupled stochastic ODEs, can be formally expressed in terms of path integrals, suggesting that it can be solved using Monte Carlo methods, by simply starting from an isotropic tetrad of radius of gyration r_0 and integrating equations (18)–(20) backwards in time, up to the time $-T$ where the norm of $|\rho|$ reaches L, the integral scale. It was found, however, that the use of straightforward Monte Carlo methods is vastly inefficient, due to the fact that few configurations contribute significantly to the solution. In practice, sampling randomly the phase space leads in the overwhelming majority of cases to insignificant contributions, the problem becoming more significant as one is interested in smaller scales.

To address this difficulty, the first attempts to solve the model used semiclassical approximation [42], with some subsequent improvements [43]. A full Monte Carlo treatment of the tetrad model has been obtained only very recently [44]. The methods used in [44] rest on the ideas of importance sampling, as well as on the "Pruned-Enriched" algorithm introduced in the context of statistical physics [45]. The main physical idea consists in identifying, as they are generated, configurations (trajectories in phase space) that are giving rise to important contributions to the computed observable, expressed as a path integral, and in sampling more in the corresponding phase space region. On the contrary, configurations that are giving very small contributions are selectively eliminated. Such methods have been successfully used in several statistical physics problems (see e.g. [46]).

We found in this problem that such methods allow us to determine efficiently the spatial dependence of the solution. Fig. 1 shows an example of the joint probability distribution function in the plane of the two invariants of the 3×3 traceless matrix $\mathbf{M}$: $Q = -\frac{1}{2}\,\mathrm{tr}(\mathbf{M}^2)$ and $R = -\frac{1}{3}\,\mathrm{tr}(\mathbf{M}^3)$. The location of the points where $\Delta = 0$ is shown in Fig. 1 as a dashed line; below this line, all eigenvalues of $\mathbf{M}$ are real; whereas above this line, one eigenvalue is real, and two are complex conjugate. This shows that regions where the flow locally rotates are above the $\Delta = 0$ line. In addition, for $R \geqslant 0$

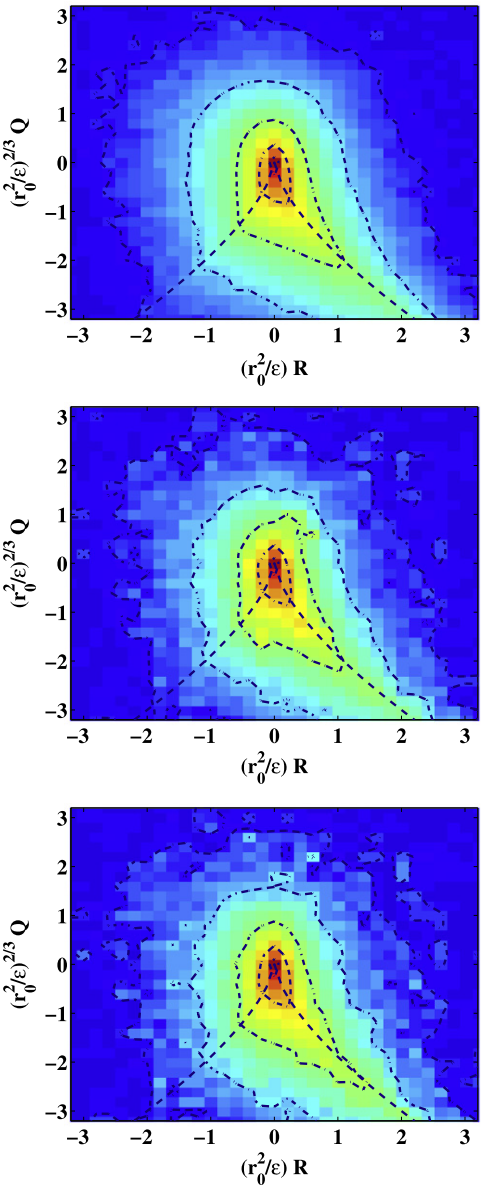

Fig. 1. Probability distribution function of the two invariants $R = -\frac{1}{3}\,\mathrm{tr}(\mathbf{M^3})$ and $Q = -\frac{1}{2}\,\mathrm{tr}(\mathbf{M^2})$ at three values of the scale r_0 of the tetrad: $r_0 = L/4$ (upper panel); $r_0 = L/16$ (middle) and $r_0 = L/64$ (lower panel). Isoprobability contours, logarithmically separated by a factor 10, are shown by the dashed-dotted lines. The zero discriminant line $4Q^3 + 27R^2 = 0$ is shown as a dashed line. The solution does not evolve much when the scale decreases. The values of the parameters are $\alpha = 0.5$, $C_\eta = 0.5$ and $C_\xi = 0.15$.

($R \leqslant 0$), two eigenvalues are positive (negative), or have positive (negative) real parts, and the third eigenvalue is negative (positive).

Fig. 1 shows the skewness already observed in DNS studies both for the velocity gradient tensor, and for the perceived velocity gradient tensor **M**. In addition, Fig. 1 shows little evolution of the PDF of R and Q when the scale r_0 diminishes. This is very suggestive of a behavior of the self-similar behavior of the flow in the inertial range of scales of the flow. The solutions of the tetrad model are shown here for one set of the parameters α, C_η and C_ξ. It was shown in [44] that the lack of symmetry $R \to -R$ of the PDF, related to the growth of probability along the $R > 0$ side of the separatrix $4Q^3 + 27R^2 = 0$, was increasingly visible for values of α decreasing from 0.9 to 0.5, and was saturating for $\alpha \lesssim 0.3$. This lack of symmetry $R \to -R$ is also strongly reduced for increasing values of C_η. The dependence of the model's solutions with respect to C_ξ has been shown to be much weaker. By using this numerical method, Pumir and Naso also found that the moments of order $n \leqslant 4$ of the solutions of the tetrad model scale with the coarse-graining length and that the scaling exponents are very close to the predictions of the Kolmogorov theory [44]. In comparison with the available (experimental or numerical) data,

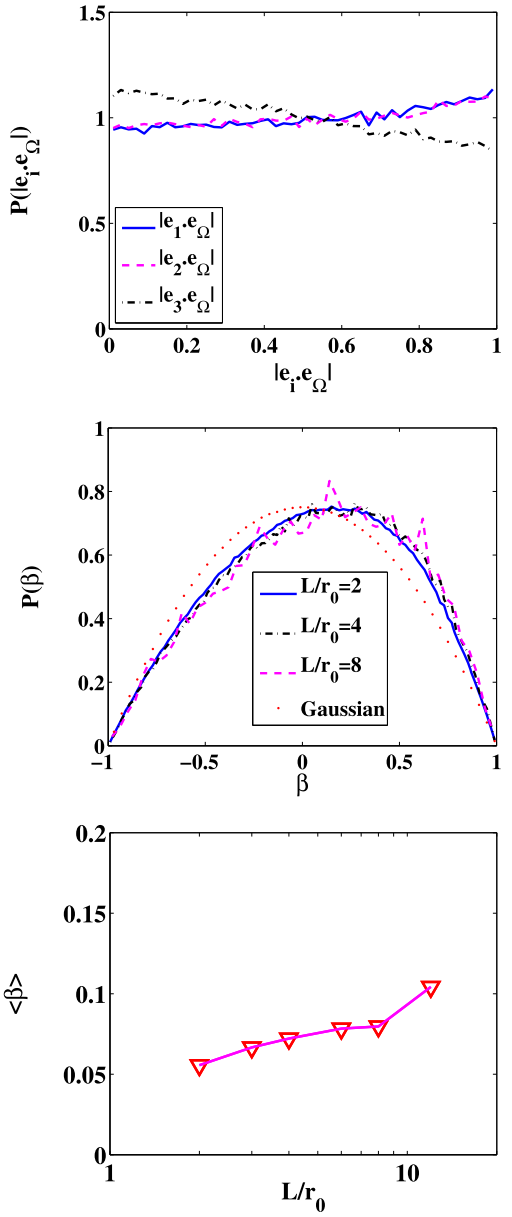

Fig. 2. Statistical properties of the vorticity and strain predicted by the model Eqs. (18), (19), (20). The upper panel shows the probability distribution of the cosines between the eigenvectors of strain, $\mathbf{e}_i$, and vorticity ($r_0 = L/4$). It shows that vorticity aligns equally well with the two eigenvectors $\mathbf{e}_1$ and $\mathbf{e}_2$. The middle panel shows the pdfs of β for three values of the tetrad size ($r_0/L = 1/2$, $1/4$ and $1/8$). For comparison, the pdf of β in the case of a Gaussian ensemble of traceless matrices $\mathbf{M}$ is shown (dotted curve). Thus, the pdf of β deviate systematically from the distribution obtained in the Gaussian case, but these deviations appear to be scale independent. Last, the lower panel shows the average of β as a function of scale, and shows a slight increase of $\langle\beta\rangle$ ($\geqslant 0$) when r_0 decreases. The values of the parameters are $\alpha = 0.5$, $C_u = 0.15$ and $C_\eta = 2$.

the model qualitatively reproduces quite well the statistics concerning the local structure of the flow. It is however found that the model generally tends to predict an excess of strain compared to vorticity.

The model also allows us to determine the properties of the strain, $\mathbf{S} = \frac{1}{2}(\mathbf{M} + \mathbf{M}^T)$ and of the vorticity, $\Omega_a = \epsilon_{abc} M_{bc}$. In fact, it has been noticed for a long time that vorticity, $\boldsymbol{\omega} = \nabla \times \mathbf{u}$ is mostly aligned with the eigenvector corresponding to the intermediate eigenvalue λ_2 of the strain [32,35]. In addition, the intermediate eigenvalue λ_2 is mostly positive. This can be seen by investigating the parameter β, defined by:

$$\beta \equiv \frac{\sqrt{6}\lambda_2}{\sqrt{\lambda_1^2 + \lambda_2^2 + \lambda_3^2}} \tag{23}$$

The value of β is in the range $-1 \leqslant \beta \leqslant 1$ when $\lambda_1 \geqslant \lambda_2 \geqslant \lambda_3$.

Fig. 2 quantifies the alignment properties of the vorticity $\mathbf{\Omega}$ with the eigenvalues of the rate of strain $\mathbf{S}$, as well as the probability distribution function of β, and its scale dependence. The upper panel shows that the model predicts a slight alignment between vorticity and the two eigenvectors of the rate of strain, corresponding to the two largest eigenvalues, which can be seen by the enhanced probability for values of $|\mathbf{e}_i \cdot \mathbf{e}_\Omega|$ close to 1. In comparison, vorticity is mostly perpendicular to the strain eigenvector corresponding to the smallest eigenvalue, $\mathbf{e}_3$. The fact that vorticity $\mathbf{\Omega}$ aligns as much with the first as the second eigenvectors of strain is a-priori surprising, as standard arguments suggest that $\mathbf{\Omega}$ should have aligned strongly with $\mathbf{e}_1$, and not so much with $\mathbf{e}_2$. However, observations both at very small scales, and more recently for r_0 in the inertial range [40], indicate that $\mathbf{\Omega}$ and $\mathbf{e}_1$ do not show any alignment at all, in the sense that the PDF of $\mathbf{e}_1 \cdot \mathbf{e}_\Omega$ is flat. On the other hand, a much stronger alignment is observed between $\mathbf{e}_2$ and $\mathbf{e}_\Omega$. The PDF shown in Fig. 2 therefore demonstrate that while the model does not quite reproduce quantitatively the observed alignment property, it does indicate that the usual casual argument that $\mathbf{\Omega}$ should be more aligned with $\mathbf{e}_1$, than with $\mathbf{e}_2$, than with $\mathbf{e}_3$ is not correct. It would be interesting to understand in more detail the alignment properties observed in the model, as it is very likely to shed light on those observed in turbulent flows.

The intermediate panel of Fig. 2 shows the PDF of β, defined by Eq. (23), for several values of the size r_0 of the tetrad, whereas the lower panel shows the averaged value $\langle\beta\rangle$ as a function of r_0. Both pictures show that β is predominantly positive: the PDF of β is skewed towards positive values. Fig. 2 also reveals that the distribution of β does not change much as a function of r_0. This very weak evolution of the statistical properties of the quantities computed with the help of the model, Eqs. (18), (19), (20), is consistent with the results obtained in [44]. More importantly, it is also indicative of the fact that the properties of alignment observed in experiments at relatively high Reynolds number ($R_\lambda \approx 350$) also suggest a very weak dependence of the properties of $\mathbf{M}$ as a function of r_0 [40].

6. Summary and conclusions

The approach discussed in this short review, based on following Lagrangian tetrads in turbulent flows, provides new insight on the structure of turbulence. In particular, varying the size r_0 of the tetrads allows us to obtain insight on the scale dependence of the flow, on its structure and topology, as well as on some important aspects of the dynamics. In relation to this approach, the model proposed originally in [22] can be solved numerically by using refined Monte Carlo techniques, using importance sampling methods. While not all the properties of the flows are quantitatively reproduced by the solutions of the model, we find that the model correctly captures some important aspects observed in experiments and in DNS, in particular those concerning the topology, and the lack of strong alignment between vorticity and the eigendirection of the rate of strain corresponding to the largest eigenvalue of $\mathbf{S}$. As observed in experiments and in DNS, the model predicts a very weak dependence of the flow properties as a function of the scale r_0 in the inertial range.

The approach presented here thus has the potential to shed light on some of the surprising properties of turbulence, and to give new information on the structure of the flow, thus providing a better understanding of the generation of small scales.

Acknowledgements

It is a pleasure to acknowledge here many discussions with E. Bodenschatz, M. Chertkov, J. Mutschall, B. Shraiman, E. Siggia and H. Xu. None of the ideas and results summarized here could have been developed without their input and continued collaboration. This work has been supported by ANR under contracts DSPET and TEC2. IDRIS has provided continuous support in terms of computer resources over the years. We have also benefited from the support of the COST Action MP0806, “Particles in Turbulence”.

References

[1] A.N. Kolmogorov, Dokl. Akad. Nauk SSSR 30 (1941) 301.
[2] G.I. Barenblatt, Ya.B. Zeldovich, Self-similar solutions as intermediate asymptotics, Ann. Rev. Fluid Mech. 4 (1972) 295.
[3] F. Anselmet, Y. Gagne, E.J. Hopfinger, R.A. Antonia, High-order velocity structure functions in turbulent shear flows, J. Fluid Mech. 140 (1984) 63.
[4] Z.S. She, E. Leveque, Universal scaling laws in fully developed turbulence, Phys. Rev. Lett. 72 (1994) 336.
[5] U. Frisch, Turbulence, Cambridge University Press, 1996.
[6] G. Falkovich, I. Fouxon, Y. Oz, New relations for correlation functions in Navier–Stokes turbulence, J. Fluid Mech. 644 (2010) 465.
[7] R. Friedrich, A. Daitche, O. Kamps, J. Lülff, M. Voßkuhle, M. Wilczek, The Lundgren–Monin–Novikov hierarchy: kinetic equations for turbulence, C. R. Phys. 13 (2012) 929–953.
[8] A. Pumir, E.D. Siggia, Collapsing solutions to the 3-D Euler equations, Phys. Fluids A 2 (1990) 220.
[9] R.M. Kerr, Evidence for a singularity of the three-dimensional incompressible Euler equations, Phys. Fluids A 5 (1993) 1725.
[10] T. Grafke, H. Homann, J. Dreher, R. Grauer, Numerical simulations of possible finite time singularities in the incompressible Euler equations: comparison of numerical methods, Physica D 237 (2008) 14.
[11] S.S. Girimaji, S.B. Pope, A diffusion model for velocity gradients in turbulence, Phys. Fluids A 2 (1990) 242.
[12] J. Martin, C. Dopazo, L. Valino, Dynamics of velocity gradient invariants in turbulence: restricted Euler and linear diffusion models, Phys. Fluids 10 (1998) 2012.
[13] E. Jeong, S.S. Girimaji, Velocity-gradient dynamics in turbulence: effect of viscosity and forcing, Theoret. Comput. Fluid Dyn. 16 (2003) 421.
[14] Y. Li, C. Meneveau, Origin of non-Gaussian statistics in hydrodynamic turbulence, Phys. Rev. Lett. 95 (2005) 164502.
[15] L. Chevillard, C. Meneveau, Lagrangian dynamics and statistical geometric structure of turbulence, Phys. Rev. Lett. 97 (2006) 174501.

[16] C. Meneveau, Lagrangian dynamics and models of the velocity gradient tensor in turbulent flows, Ann. Rev. Fluid Mech. 43 (2011) 219.
[17] F. van der Bos, B. Tao, C. Meneveau, J. Katz, Effects of small-scale turbulent motions on the filtered velocity gradient tensor as deduced from holographic particle image velocimetry measurements, Phys. Fluids 14 (2002) 2457.
[18] B.W. Zeff, D.D. Lanterman, R. McAllister, R. Roy, E.J. Kostelich, D.P. Lathrop, Measuring intense rotation and dissipation in turbulent flows, Nature 421 (2003) 146.
[19] L. Mydlarski, A. Pumir, B. Shraiman, E.D. Siggia, Z. Warhaft, Structures and multipoint correlators for turbulent advection: predictions and experiments, Phys. Rev. Lett. 81 (2008) 4373.
[20] B.I. Shraiman, E.D. Siggia, Scalar turbulence, Nature 405 (2000) 639.
[21] Z. Warhaft, Passive scalars in turbulent flows, Ann. Rev. Fluid Mech. 32 (2000) 203.
[22] M. Chertkov, A. Pumir, B.I. Shraiman, Lagrangian tetrad dynamics and the phenomenology of turbulence, Phys. Fluids 11 (1999) 2394.
[23] R.H. Kraichnan, Convection of a passive scalar by a quasi uniform random straining field, J. Fluid Mech. 64 (1974) 737.
[24] B.I. Shraiman, E.D. Siggia, Anomalous scaling of a passive scalar in turbulent flow, C. R. Acad. Sci. Ser. II, Paris 321 (1995) 279.
[25] G. Falkovich, K. Gawedzki, M. Vergassola, Particles and fields in fluid turbulence, Rev. Mod. Phys. 73 (2001) 913, is that the Lagrangian point of view.
[26] W.H. Press, S.A. Teukolsky, W.T. Vetterling, B.P. Flannery, Numerical Recipes in Fortran 77, Cambridge University Press, 1992.
[27] B.J. Cantwell, On the behavior of velocity gradient tensor invariants in direct numerical simulations of turbulence, Phys. Fluids A 5 (1993) 2008.
[28] A. Pumir, B.I. Shraiman, M. Chertkov, Geometry of Lagrangian dispersion in turbulence, Phys. Rev. Lett. 85 (2000) 5324.
[29] L. Biferale, G. Boffetta, A. Celani, B.J. Devenish, A. Lanotte, F. Toschi, Multiparticle dispersion in fully developed turbulence, Phys. Fluids 17 (2005) 111701.
[30] H. Xu, N.T. Ouellette, E. Bodenschatz, Evolution of geometric structures in intense turbulence, New J. Phys. 10 (2008) 013012.
[31] J.F. Hackl, P.K. Yeung, B.L. Sawford, Multi-particle and tetrad statistics in numerical simulations of turbulent relative dispersion, Phys. Fluids 23 (2011) 065103.
[32] E.D. Siggia, Invariants for the one-point vorticity and strain rate correlation functions, Phys. Fluids (1981) 1934.
[33] K.K. Nomura, G.K. Post, The structure and dynamics of vorticity and rate of strain in incompressible homogeneous turbulence, J. Fluid Mech. 377 (1998) 65.
[34] M. Guala, B. Luthi, A. Liberzon, A. Tsinober, W. Kinzelbach, On the evolution of material lines and vorticity in homogeneous turbulence, J. Fluid Mech. 533 (2005) 339.
[35] Wm.T. Ashurst, A.R. Kerstein, R.M. Kerr, C.H. Gibson, Alignment of vorticity and scalar gradient with strain rate in simulated Navier–Stokes turbulence, Phys. Fluids (1987) 2343.
[36] Z.S. She, E. Jackson, S.A. Orszag, Structure and dynamics of homogeneous turbulence. Models and simulations, Proc. R. Soc. Lond. A 434 (1991) 101.
[37] A. Tsinober, E. Kit, T. Dracos, Experimental investigation of the field of velocity gradients in turbulent flows, J. Fluid Mech. 242 (1992) 169.
[38] H. Xu, A. Pumir, E. Bodenschatz, The Pirouette effect in turbulent flows, Nat. Phys. 7 (2011) 709.
[39] L. Chevillard, C. Meneveau, Lagrangian time correlations of vorticity alignments in isotropic turbulence: observations and model predictions, Phys. Fluids 23 (2011) 101704.
[40] A. Pumir, E. Bodenschatz, H. Xu, Tetrahedron deformation and alignment of perceived velocity and strain in a turbulent flow, Phys. Fluids (2012), submitted for publication, arXiv:1204.5857.
[41] H. Tennekes, J.L. Lumley, A First Course in Turbulence, MIT Press, Cambridge, 1972.
[42] A. Naso, A. Pumir, Scale dependence of the coarse-grained velocity derivative tensor structure in turbulence, Phys. Rev. E 72 (2005) 056318.
[43] A. Naso, A. Pumir, M. Chertkov, Statistical geometry in homogeneous and isotropic turbulence, J. Turbul. 8 (2007) 39.
[44] A. Pumir, A. Naso, Statistical properties of the coarse-grained velocity gradient tensor in turbulence: Monte Carlo simulations of the tetrad model, New J. Phys. 12 (2010) 123024.
[45] P. Grassberger, Pruned-enriched Rosenbluth method: simulation of θ-polymers of chain length up to 1 000 000, Phys. Rev. E 56 (1997) 3682.
[46] D.A. Adams, L.M. Sander, R.M. Ziff, The barrier method: a technique for calculating very long transition times, J. Chem. Phys. 41 (2010) 8.